Cooperative quantum jumps for three dipole-interacting atoms

Volker Hannstein and Gerhard C. Hegerfeldt
Institut für Theoretische Physik, Universität Göttingen, Tammannstraße 1, 37077 Göttingen, Germany
(Received 12 December 2003; published 30 August 2004)

We investigate the effect of the dipole-dipole interaction on the quantum jump statistics of three atoms. This is done for three-level systems in a V configuration and in what may be called a D configuration. The transition rates between the four different intensity periods are calculated in closed form. Cooperative effects are shown to increase by a factor of 2 compared to two of either three-level systems. This results in transition rates that are, for distances of about one wavelength of the strong transition, up to 100% higher than for independent systems. In addition the double and triple jump rates are calculated from the transition rates. In this case cooperative effects of up to 170% for distances of about one wavelength and still up to 15% around 10 wavelengths are found. Nevertheless, for the parameters of an experiment with Hg^+ ions the effects are negligible, in agreement with the experimental data. For three Ba^+ ions this seems to indicate that the large cooperative effects observed experimentally cannot be explained by the dipole-dipole interaction.

DOI: 10.1103/PhysRevA.70.023820 PACS number(s): 42.50.Ct, 42.50.Ar, 42.50.Fx

I. INTRODUCTION

Cooperative effects due to the dipole-dipole interaction between atoms are of great importance in many fields, most recently in the study of possible quantum computers based on trapped ions or atoms, and therefore they have attracted considerable interest in the literature [1]. A sensitive test for such cooperative effects can be provided by atoms showing macroscopic light and dark periods in their fluorescence. These can occur in a multilevel system if the electron is essentially shelved in a metastable state, thereby causing the photon emission to cease [2]. Two or three such systems accordingly show three or four periods of different intensity, namely one dark period and bright periods with once, twice, or three times the intensity of a single system's bright period. The dipole-dipole interaction may alter the statistics of these periods. In an as yet unexplained experiment with two and three Ba^+ ions [3,4] a large number of double and triple jumps, i.e., jumps by two or three intensity steps within a short resolution time, was observed, exceeding by far the value expected for independent atoms. The quantitative explanation of such large cooperative effects for distances of the order of 10 wavelengths of the strong transition has been found difficult [5–10]. Experiments with other ions showed no observable cooperative effects [11,12], in particular none were seen for Hg^+ for a distance of about 15 wavelengths [13]. More recently effects similar to Ref. [3] were found in an experiment with Ca^+ ions [14] in contrast to a comparable experiment [15]. A different method for observing the dipole-dipole interaction of two V systems was proposed in Ref. [16].

The effect of the dipole–dipole interaction for two V systems was investigated numerically in Ref. [17] and analytically in Ref. [18] and shown to be up to 30% in the double jump rate compared to independent systems. However, the systems used in the experimental setups of Refs. [3,13,19] cannot be described by a V system so that a direct comparison between theory and experiment was not possible. For this reason the present authors have investigated cooperative effects for two other systems [20], namely a D shaped system modeling the Hg^+ ions used in Ref. [13] and a four-level system modeling the Ba^+ ions of Refs. [3,4]. For two D systems cooperative effects in the same order of magnitude as for the V systems were found for ion distances of a few wavelengths of the laser-driven transition. For larger distances practically no effects where found, in agreement with the experiments [13] and with the results of Ref. [21]. In contrast, only negligible effects for arbitrary ion distances were found for two of the four level systems. Although this result contradicts the findings of Refs. [3,4] a direct quantitative comparison with the experiments was not possible since explicit experimental data were only provided for three Ba^+ ions.

The aim of this paper is to narrow this gap by investigating *three* dipole-interacting three-level systems in a V configuration and in a D configuration (see Figs. 1 and 2), respectively, and to compare the results with those for two such systems. For three system this becomes much more complicated since one has to deal with 729×729 matrices, and in order to do this we use group theoretical methods to exploit the symmetry of the problem.

We calculate the transition rates between the different intensity periods for both systems. Cooperative effects are found to increase by a factor of 2 in the first order terms in the interaction parameter C_3 when compared to two of either systems. This results in transition rates up to 100% higher than the rates for independent systems. We also calculate the double and triple jump rates for both systems. Here the cooperative effects are even larger.

A full description of the Ba^+ experiment [3,4] would require the treatment of three of the four-level systems of Ref.

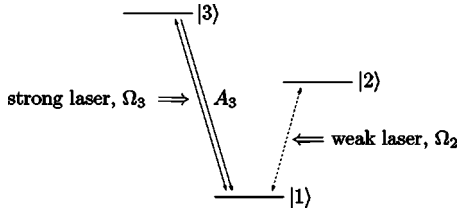

FIG. 1. Three-level system in V configuration.

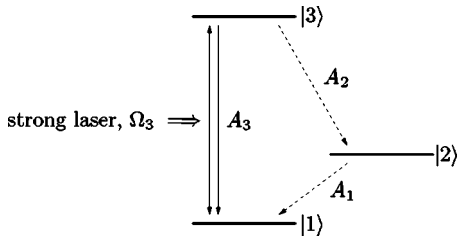

FIG. 2. Three-level system in D configuration with fast transitions (solid lines) and slow transitions (dashed lines).

[20]. However, here we will restrict ourselves to the three-level systems, since this reduces the complexity of the calculation considerably. Also, the similarities between the results for the D system and the four-level system pointed out in Ref. [20] seem to allow to draw conclusions on the cooperative behavior of three four-level systems from the results presented here. Namely, the increase of cooperative effects is not strong enough to yield significant effects for three four-level systems.

Section II deals with the main assumptions of the models. In Sec. III the methods for the calculation of the transition rates first for the V systems and afterwards for the D system are explained. In Sec. IV the results of the calculations are presented, namely the transition rates between the different intensity periods. Finally in Sec. V the double and triple jump rates are calculated from the transition rates. The results are discussed and compared with those of two three-level systems.

II. DIPOLE-INTERACTING THREE-LEVEL SYSTEMS

In the following we investigate three dipole-interacting-three-level systems both in a V-type and in a D-type configuration as shown in Figs. 1 and 2. For the V system the Rabi frequencies Ω_2 and Ω_3 and the Einstein coefficient A_3 satisfy

$$\Omega_3, A_3 \gg \Omega_2 \tag{1}$$

so that the single system can show macroscopic light and dark periods. The D system exhibits the same property if the condition

$$\Omega_3, A_3 \gg A_1, A_2 \tag{2}$$

for the Einstein coefficients and the Rabi frequency is fulfilled. We assume the three atoms to be at fixed positions forming an equilateral triangle, in agreement with the experimental setups. Furthermore, for simplicity, the direction of the laser beams are assumed to be perpendicular to the plane of this triangle.

The Bloch equation can be written in the form [22]

$$\dot{\rho} = -\frac{\mathrm{i}}{\hbar}[H_{\mathrm{cond}}\rho - \rho H_{\mathrm{cond}}^{\dagger}] + \mathcal{R}(\rho), \tag{3}$$

where the conditional Hamiltonian H_{cond} and the reset operation $\mathcal{R}(\rho)$ for a general three-level system are given by [23,24]

$$H_{\mathrm{cond}} = \sum_{i=1}^{3}\sum_{j=1}^{3}\frac{\hbar}{2\mathrm{i}}A_j S_{ij}^{+}S_{ij}^{-} + \sum_{i=1}^{3}\sum_{j=2}^{3}\frac{\hbar}{2}[\Omega_j S_{ij}^{-} + \mathrm{H.c.}] + \sum_{\substack{k,l=1 \\ k<l}}^{3}\sum_{j=1}^{3}\frac{\hbar}{2\mathrm{i}}C_{kl}^{(j)}(S_{kj}^{+}S_{lj}^{-} + S_{lj}^{+}S_{kj}^{-}) \tag{4}$$

and

$$\mathcal{R}(\rho) = \sum_{i=1}^{3}\sum_{j=1}^{3}A_j S_{ij}^{-}\rho S_{ij}^{+} + \sum_{\substack{k,l=1 \\ k<l}}^{3}\sum_{j=1}^{3}\mathrm{Re}\, C_{kl}^{(j)}(S_{kj}^{-}\rho S_{lj}^{+} + S_{lj}^{-}\rho S_{kj}^{+}), \tag{5}$$

with

$$S_{i1}^{+} = |2\rangle_{ii}\langle 1|, \quad S_{i2}^{+} = |3\rangle_{ii}\langle 2|,$$

$$S_{i3}^{+} = |3\rangle_{ii}\langle 1|, \quad \text{and } S_{ij}^{-} = S_{ij}^{+\dagger}. \tag{6}$$

Here,

$$C_{kl}^{(j)} = \frac{3A_j}{2}e^{ia_{kl}^{(j)}}\left[\frac{1}{ia_{kl}^{(j)}}(1-\cos^2\theta_{kl}) + \left(\frac{1}{a_{kl}^{(j)2}} - \frac{1}{ia_{kl}^{(j)3}}\right)(1-3\cos^2\theta_{kl})\right] \tag{7}$$

is the coupling parameter which describes the dipole-dipole interaction between atom k and atom l for the transition connected with the Einstein coefficient A_j, with θ_{kl} being the angle between the dipole moments and the line connecting the atoms. The dimensionless parameter $a_{kl}^{(j)} = 2\pi r_{kl}/\lambda_j$ is given by the interatomic distance r_{kl} multiplied by the wave number $2\pi/\lambda_j$ of this transition. The detunings of the lasers are taken as zero. By setting either $A_1 = A_2 = C_{kl}^{(1)} = C_{kl}^{(2)} = 0$ or $\Omega_2 = 0$ in Eqs. (4) and (5) the Hamiltonians and reset states for the V systems and the D systems, respectively, are obtained. For simplicity it would be preferable to have the same coupling parameters for each pair of atoms (i.e., $C_{kl}^{(j)} \equiv C_j$). This would be the case if the angle between the dipole moments and the line connecting two atoms were the same for all pairs of atoms. However, the arrangement of the atoms in the trap makes this impossible, as is illustrated in Fig. 3. The atoms form an equilateral triangle (i.e., $r_{kl} = r$) with the laser beams perpendicular to the plane of this triangle and the dipole moments aligned by a magnetic field in a direction in this plane. In this situation, the same value of the coupling constants can only be achieved for two of the three possible pairs of atoms. However, in spite of this we will assume $C_{kl}^{(j)} \equiv C_j$ because this case leads to maximal cooperative effects and can be seen as a limiting case for all other possible configurations. The reset state can then be written as a sum of density matrices of pure states

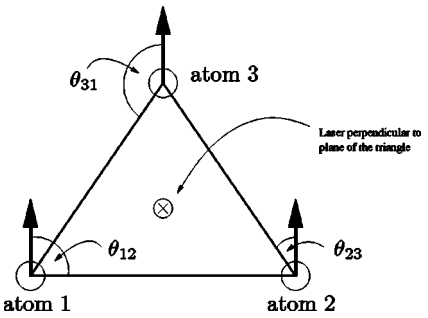

FIG. 3. Geometry of the atoms in the trap. The arrows symbolize the dipole moments. In the picture the angles have the values $\theta_{12}=\pi/2$, $\theta_{23}=\pi/6$, and $\theta_{31}=5\pi/6$ leading to $\cos^2\theta_{12}=0$, and $\cos^2\theta_{23}=\cos^2\theta_{31}=3/4$.

$$\mathcal{R}(\rho)=\sum_{j=1}^{3}\{(A_j+2\ \mathrm{Re}\ C_j)R_1^{(j)}\rho R_1^{(j)\dagger}+(A_j-\mathrm{Re}\ C_j)[R_2^{(j)}\rho R_2^{(j)\dagger}+R_3^{(j)}\rho R_3^{(j)\dagger}]\}, \tag{8}$$

with

$$R_1^{(j)}=\frac{1}{\sqrt{3}}(S_{1j}^-+S_{2j}^-+S_{3j}^-),$$

$$R_2^{(j)}=\frac{1}{\sqrt{6}}(2S_{1j}^--S_{2j}^--S_{3j}^-),$$

$$R_3^{(j)}=\frac{1}{\sqrt{2}}(S_{2j}^--S_{3j}^-). \tag{9}$$

In the case of two systems, it was convenient to use a Dicke basis, i.e., a basis consisting of the symmetric and antisymmetric linear combinations of the product states. Generally speaking, this means using a basis which is adapted with respect to the symmetry group S_2 of permutations of two atoms. The symmetric and antisymmetric states correspond to the irreducible representations of this group. For three three-level systems, we therefore use a basis that is adapted to the symmetry group S_3 of permutations of three particles. On the subspace spanned by the product states with all three atoms in different states the irreducible representations of the S_3 are the two one-dimensional representations mentioned above and another two equivalent two-dimensional representations. This leads to the states

$$|s_{123}\rangle=\frac{1}{\sqrt{6}}(|1\rangle|2\rangle|3\rangle+|2\rangle|3\rangle|1\rangle+|3\rangle|1\rangle|2\rangle+|1\rangle|3\rangle|2\rangle+|2\rangle|1\rangle|3\rangle+|3\rangle|2\rangle|1\rangle), \tag{10a}$$

$$|a_{123}\rangle=\frac{1}{\sqrt{6}}(|1\rangle|2\rangle|3\rangle+|2\rangle|3\rangle|1\rangle+|3\rangle|1\rangle|2\rangle-|1\rangle|3\rangle|2\rangle-|2\rangle|1\rangle|3\rangle-|3\rangle|2\rangle|1\rangle), \tag{10b}$$

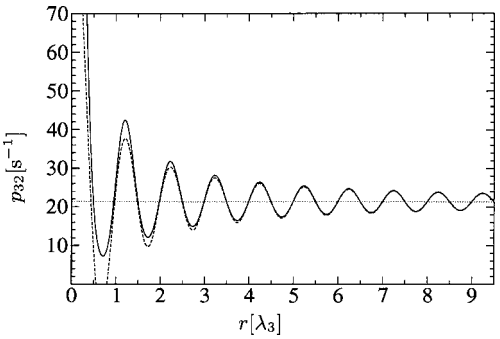

FIG. 4. Transition rate p_{32} for three dipole-interacting V systems plotted versus the interatomic distance r in units of the wavelength λ_3 of the strong transition. Solid line, p_{32} up to second order in C_3. Dashed line, first order. Dotted line, independent systems. Parameter values are $A_3=2\times10^8\ s^{-1}$, $\Omega_3=5\times10^7\ s^{-1}$, and $\Omega_2=10^4\ s^{-1}$.

$$|b_{123}\rangle=\frac{1}{\sqrt{12}}(2|1\rangle|2\rangle|3\rangle-|2\rangle|3\rangle|1\rangle-|3\rangle|1\rangle|2\rangle+2|1\rangle|3\rangle|2\rangle-|2\rangle|1\rangle|3\rangle-|3\rangle|2\rangle|1\rangle), \tag{10c}$$

$$|c_{123}\rangle=\tfrac{1}{2}(|2\rangle|3\rangle|1\rangle-|3\rangle|1\rangle|2\rangle-|2\rangle|1\rangle|3\rangle+|3\rangle|2\rangle|1\rangle), \tag{10d}$$

$$|d_{123}\rangle=\frac{1}{\sqrt{12}}(2|1\rangle|2\rangle|3\rangle-|2\rangle|3\rangle|1\rangle-|3\rangle|1\rangle|2\rangle-2|1\rangle|3\rangle|2\rangle+|2\rangle|1\rangle|3\rangle+|3\rangle|2\rangle|1\rangle), \tag{10e}$$

$$|e_{123}\rangle=\tfrac{1}{2}(|2\rangle|3\rangle|1\rangle-|3\rangle|1\rangle|2\rangle+|2\rangle|1\rangle|3\rangle-|3\rangle|2\rangle|1\rangle) \tag{10f}$$

in the case where all three atoms are in different states. For the remaining states one then easily gets for $i,j=1,2,3$, $i\neq j$,

$$|s_{ijj}\rangle=\frac{1}{\sqrt{3}}(|i\rangle|j\rangle|j\rangle+|j\rangle|j\rangle|i\rangle+|j\rangle|i\rangle|j\rangle), \tag{11a}$$

$$|b_{ijj}\rangle=\frac{1}{\sqrt{6}}(2|i\rangle|j\rangle|j\rangle-|j\rangle|j\rangle|i\rangle-|j\rangle|i\rangle|j\rangle), \tag{11b}$$

$$|c_{ijj}\rangle=\frac{1}{\sqrt{2}}(|j\rangle|j\rangle|i\rangle-|j\rangle|i\rangle|j\rangle), \tag{11c}$$

if two atoms are in the same state and

$$|g\rangle=|1\rangle|1\rangle|1\rangle,\quad |e_2\rangle=|2\rangle|2\rangle|2\rangle,\quad |e_3\rangle=|3\rangle|3\rangle|3\rangle \tag{12}$$

if all three atoms are in the same state.

III. TRANSITION RATES

For the calculation of the transition rates, we carry over the methods that have already been used for the description of two dipole-interacting V systems and D systems, respectively [18,20].

For both types of systems, the configuration decouples into four independent subspaces if one neglects the small parameters (i.e., $\Omega_2=0$ for the V systems and $A_1=A_2=0$ for the D systems)

$$\mathcal{S}_0=\{|e_2\rangle\}, \tag{13a}$$

$$\mathcal{S}_1=\{|s_{122}\rangle,|b_{122}\rangle,|c_{122}\rangle,|s_{322}\rangle,|b_{322}\rangle,|c_{322}\rangle\}, \tag{13b}$$

$$\mathcal{S}_2=\{|s_{211}\rangle,|b_{211}\rangle,|c_{211}\rangle,|s_{123}\rangle,|a_{123}\rangle|b_{123}\rangle,|c_{123}\rangle,|d_{123}\rangle,|e_{123}\rangle,|s_{233}\rangle,|b_{233}\rangle,|c_{233}\rangle\}, \tag{13c}$$

$$\mathcal{S}_3=\{|g\rangle,|s_{311}\rangle,|b_{311}\rangle,|c_{311}\rangle,|s_{133}\rangle,|b_{133}\rangle,|c_{133}\rangle,|e_3\rangle\}, \tag{13d}$$

in analogy to the case of two of either systems. In a period of intensity I_i, the density matrix of the system is mostly in subspace $\mathcal{S}_i$ [25]. The transition rates will thus be calculated by using a density matrix in one particular subspace and then the rate of build-up of population in another subspace will be determined.

Taking a state $\rho_{0,i}$ in one of the subspaces $\mathcal{S}_i$ at a time t_0 we calculate the state after a time $t_0+\Delta t$ in perturbation theory with respect to the small parameters. The time interval used here should be long in comparison to the mean time between the emission of two photons but short in comparison to the length of the intensity periods,

$$A_3^{-1},\Omega_3^{-1}\ll\Delta t\ll\Omega_2^{-1}\quad(\text{V system}),$$

$$A_3^{-1},\Omega_3^{-1}\ll\Delta t\ll A_1^{-1},A_2^{-1}\quad(\text{D system}). \tag{14}$$

For the calculation the Bloch equation is written in a Liouvillean form

$$\dot{\rho}=\mathcal{L}\rho=\{\mathcal{L}_0(A_3,C_3,\Omega_3)+\mathcal{L}_1\}\rho, \tag{15}$$

where $\mathcal{L}_1$ serves as the perturbation depending on Ω_2 or A_1, A_2, C_1, and C_2, respectively. We then get [18]

$$\rho(t_0+\Delta t;\rho_{\mathrm{ss},i})=\rho_{\mathrm{ss},i}+\int_0^{\Delta t}d\tau\, e^{\mathcal{L}_0\tau}\mathcal{L}_1\rho_{\mathrm{ss},i}, \tag{16}$$

where $\rho_{\mathrm{ss},i}$ is the quasisteady state in subsystem $\mathcal{S}_i$. As a Liouvillean of Bloch equations, $\mathcal{L}_0$ has an eigenvalue 0 corresponding to the quasisteady states. The other eigenvalues have negative real parts of the order of Ω_3 and A_3. While $\mathcal{L}_1\rho_{\mathrm{ss},i}$ is a superposition of just the eigenstates for nonzero eigenvalues of $\mathcal{L}_0$ in the case of three V systems this is not true for three D systems, which makes it necessary to discuss the two cases separately.

A. Three V systems

For the V systems, $\mathcal{L}_1\rho_{\mathrm{ss},i}$ consists only of coherences between the subspace $\mathcal{S}_i$ and the neighboring subspaces, since $\mathcal{L}_1$ describes the coupling due to the weak laser (with Rabi frequency Ω_2) in this case. The zero-eigenvalue subspace of $\mathcal{L}_0$, on the other hand, is spanned by the quasisteady states $\rho_{\mathrm{ss},i}$. Therefore, $\mathcal{L}_1\rho_{\mathrm{ss},i}$ has no components in the zero eigenvalue subspace of $\mathcal{L}_0$ in the case of V systems. The other eigenvalues all have negative real parts of the order of A_3 and Ω_3. Therefore the integrand in Eq. (16) is rapidly damped which allows us to extend the upper integration limit to infinity. This yields

$$\rho(t_0+\Delta t;\rho_{\mathrm{ss},i})=\rho_{\mathrm{ss},i}+(\epsilon-\mathcal{L}_0)^{-1}\mathcal{L}_1\rho_{\mathrm{ss},i}, \tag{17}$$

independent of Δt [18].

From the Bloch equations (3) we get the exact relations

$$\frac{d}{dt}\langle e_2|\rho|e_2\rangle=\sqrt{3}\Omega_2\,\mathrm{Im}\langle s_{122}|\rho|e_2\rangle, \tag{18a}$$

$$\frac{d}{dt}\sum_{x_i\in S_1}\langle x_i|\rho|x_i\rangle=\Omega_3\,\mathrm{Im}\Big[2\langle s_{112}|\rho|s_{122}\rangle-\langle b_{112}|\rho|b_{122}\rangle-\langle c_{112}|\rho|c_{122}\rangle-\sqrt{3}\langle s_{122}|\rho|e_2\rangle+\sqrt{2}\langle s_{123}|\rho|s_{223}\rangle-\frac{1}{\sqrt{2}}(\langle b_{123}|\rho|b_{223}\rangle$$
$$+\langle c_{123}|\rho|c_{223}\rangle)+\sqrt{\frac{3}{2}}(\langle d_{123}|\rho|c_{223}\rangle-\langle e_{123}|\rho|b_{223}\rangle)\Big]-\frac{d}{dt}\langle e_2|\rho|e_2\rangle, \tag{18b}$$

$$\frac{d}{dt}\sum_{x_i\in S_2}\langle x_i|\rho|x_i\rangle = -\Omega_3\,\mathrm{Im}\Big[2\langle s_{112}|\rho|s_{122}\rangle - \langle b_{112}|\rho|b_{122}\rangle - \langle c_{112}|\rho|c_{122}\rangle - \sqrt{3}\langle s_{122}|\rho|e_2\rangle + \sqrt{2}\langle s_{123}|\rho|s_{223}\rangle - \frac{1}{\sqrt{2}}(\langle b_{123}|\rho|b_{223}\rangle + \langle c_{123}|\rho|c_{223}\rangle) + \sqrt{\frac{3}{2}}(\langle d_{123}|\rho|c_{223}\rangle - \langle e_{123}|\rho|b_{223}\rangle)\Big] - \frac{d}{dt}\sum_{x_i\in S_3}\langle x_i|\rho|x_i\rangle, \tag{18c}$$

$$\frac{d}{dt}\sum_{x_i\in S_3}\langle x_i|\rho|x_i\rangle = \Omega_2\,\mathrm{Im}\Big[\frac{1}{\sqrt{2}}(\langle b_{113}|\rho|b_{123}\rangle + \langle c_{311}|\rho|c_{123}\rangle) + \sqrt{\frac{3}{2}}(\langle b_{311}|\rho|e_{123}\rangle - \langle c_{311}|\rho|d_{123}\rangle) - \sqrt{3}\langle g|\rho|s_{211}\rangle - \sqrt{2}\langle s_{311}|\rho|s_{233}\rangle - (\langle s_{133}|\rho|s_{233}\rangle + \langle b_{133}|\rho|b_{233}\rangle + \langle c_{133}|\rho|c_{233}\rangle)\Big]. \tag{18d}$$

Together with Eq. (17) this allows us to calculate the transition rates as

$$p_{ij} = \frac{d}{dt}\sum_{x_k\in S_j}\langle x_k|\rho|x_k\rangle\Big|_{\rho=\rho(t_0+\Delta t;\rho_{\mathrm{ss},i})}. \tag{19}$$

Note that $p_{ij}=0$ for $|i-j|\geqslant 2$ so that no *direct*, i.e., instantaneous, double jumps occur.

B. Three D systems

In the case of D systems, $\mathcal{L}_1$ describes spontaneous emission due to the Einstein coefficients A_1 and A_2. Therefore $\mathcal{L}_1\rho_{\mathrm{ss},i}$ consists of density matrix elements $\langle x_i|\rho|x_j\rangle$ where both states $|x_i\rangle$ and $|x_j\rangle$ lie in the same subspace $\mathcal{S}_i$. It is thus a superposition of eigenstates of $\mathcal{L}_0$ with zero as well as nonzero eigenvalues. We write

$$\mathcal{L}_1\rho_{\mathrm{ss},i} = \sum_{j=0}^{3}\alpha_{ij}\rho_{\mathrm{ss},j} + \tilde{\rho}, \tag{20}$$

where $\tilde{\rho}$ contains the contributions from the eigenstates for nonzero eigenvalues of $\mathcal{L}_0$. The coefficients α_{ij} are calculated by means of the dual eigenstates ρ_{ss}^{i} [20],

$$\alpha_{ij} = \mathrm{Tr}(\rho_{\mathrm{ss}}^{j\dagger}\mathcal{L}_1\rho_{\mathrm{ss},i}). \tag{21}$$

Inserting Eq. (20) into Eq. (16) one obtains

$$\rho(t_0+\Delta t) = \rho_{\mathrm{ss},i} + \sum_{j=0}^{3}\alpha_{ij}\rho_{\mathrm{ss},j}\Delta t + (\varepsilon - L_0)^{-1}\tilde{\rho}. \tag{22}$$

The last term is much smaller than the preceding term and can be neglected [20]. The coefficients α_{ij} can then be interpreted as the transition rates between the subspaces $\mathcal{S}_i$ and $\mathcal{S}_j$,

$$p_{ij} = \alpha_{ij}. \tag{23}$$

C. Group theory

For the calculation of the transition rates for both V systems and D systems it is necessary to calculate the quasisteady states $\rho_{\mathrm{ss},i}$, i.e., to solve the linear equation

$$\mathcal{L}_0\rho_{\mathrm{ss}} = 0. \tag{24}$$

In addition, for V systems the first order term

$$\rho_i^{(1)} = (\epsilon - \mathcal{L}_0)^{-1}\mathcal{L}_1\rho_{\mathrm{ss},i}$$

of Eq. (17) must be calculated, which was done by solving

$$\mathcal{L}_0\rho_i^{(1)} = \mathcal{L}_1\rho_{\mathrm{ss},i}. \tag{25}$$

Equations (24) and (25) are linear equations for the 729 matrix elements of $\rho_{\mathrm{ss},i}$ and $\rho_i^{(1)}$, respectively. Luckily there are two different properties of $\mathcal{L}_0$ that make it possible to restrict these equations to smaller subspaces, which reduces the calculation effort considerably. First, $\mathcal{L}_0$ is independent of the small parameters (A_1, A_2 or Ω_2), which means that there is no coupling between the four subspaces of Eq. (13). Thus there exist 16 subspaces $\mathcal{R}_{i,j}$, each consisting of the density matrix elements

$$\langle x_i|\rho|y_j\rangle \text{ with } |x_i\rangle\in S_i \text{ and } |y_j\rangle\in S_j, \tag{26}$$

respectively, which are invariant with respect to $\mathcal{L}_0$. In addition the conditional Hamiltonian H_{cond} and the reset state $\mathcal{R}(\rho)$ and therefore also $\mathcal{L}_0$ are invariant under the exchange of atoms, as can be seen from Eqs. (4) and (5). Hence subspaces which consist of all density matrix elements which belong to a particular irreducible representation of $\mathcal{S}_3$ are also invariant with respect to $\mathcal{L}_0$. Since the density matrix elements form a representation of $\mathcal{S}_3$ which is a tensor product of twice the representation spanned by the Dicke basis of Eq. (10) the new irreducible representations are easily found. The density matrix elements

$$|s_\alpha\rangle\langle s_\beta|, \quad |a_\alpha\rangle\langle a_\beta|,$$

$$\tfrac{1}{2}(|b_\alpha\rangle\langle b_\beta| + |c_\alpha\rangle\langle c_\beta|), \quad \tfrac{1}{2}(|d_\alpha\rangle\langle d_\beta| + |e_\alpha\rangle\langle e_\beta|),$$

$$\tfrac{1}{2}(|b_\alpha\rangle\langle e_\beta| - |c_\alpha\rangle\langle d_\beta|), \quad \tfrac{1}{2}(|e_\alpha\rangle\langle b_\beta| - |d_\alpha\rangle\langle c_\beta|) \tag{27}$$

belong to the symmetric representation, the elements

$$|s_\alpha\rangle\langle a_\beta|, \quad |a_\alpha\rangle\langle s_\beta|,$$

$$\tfrac{1}{2}(|b_\alpha\rangle\langle c_\beta| - |c_\alpha\rangle\langle b_\beta|), \quad \tfrac{1}{2}(|d_\alpha\rangle\langle e_\beta| - |e_\alpha\rangle\langle d_\beta|),$$

$$\tfrac{1}{2}(|b_\alpha\rangle\langle d_\beta| + |c_\alpha\rangle\langle e_\beta|), \quad \tfrac{1}{2}(|d_\alpha\rangle\langle b_\beta| + |e_\alpha\rangle\langle c_\beta|) \tag{28}$$

belong to the antisymmetric representation, and the remaining 24 possible linear combinations form two-dimensional representations. Here α and β are one of the subscripts of the Dicke states. By transforming the Liouvillean $\mathcal{L}_0$ into this new basis each of the 16 invariant subspaces $\mathcal{R}_{i,j}$ is in itself decomposed into three invariant subspaces connected to the elements belonging to the symmetric, antisymmetric, and two-dimensional representations, respectively. For the calculation of both the quasisteady states $\rho_{\mathrm{ss},i}$ and the transition rates for the V systems only the symmetric subspaces are needed. For the latter this can be seen from Eq. (18). With these two simplifications the dimension of the linear system of equations needed for the calculation reduces considerably (namely to a maximum of 20 for the calculation of p_{23} and p_{32}).

IV. RESULTS

The transition rates for the V systems can now be calculated according to Eqs. (19), (16), and (18). The result is

$$p_{01} = 3\frac{A_3\Omega_2^2}{\Omega_3^2}, \tag{29a}$$

$$p_{10} = \frac{A_3^3\Omega_2^2}{\Omega_3^2(A_3^2+2\Omega_3^2)}, \tag{29b}$$

$$p_{12} = 2\frac{A_3\Omega_2^2}{\Omega_3^2}\left[1 + 2\,\mathrm{Re}\,C_3\frac{A_3}{A_3^2+2\Omega_3^2}\right], \tag{29c}$$

$$p_{21} = 2\frac{A_3^3\Omega_2^2}{\Omega_3^2(A_3^2+2\Omega_3^2)}\left[1 + 2\,\mathrm{Re}\,C_3\frac{A_3(A_3^2+4\Omega_3^2)}{(A_3^2+2\Omega_3^2)^2}\right], \tag{29d}$$

$$p_{23} = \frac{A_3\Omega_2^2}{\Omega_3^2}\left[1 + 4\,\mathrm{Re}\,C_3\frac{A_3}{A_3^2+2\Omega_3^2}\right], \tag{29e}$$

$$p_{32} = 3\frac{A_3^3\Omega_2^2}{\Omega_3^2(A_3^2+2\Omega_3^2)}\left[1 + 4\,\mathrm{Re}\,C_3\frac{A_3(A_3^2+4\Omega_3^2)}{(A_3^2+2\Omega_3^2)^2}\right] \tag{29f}$$

to first order in C_3. While for p_{01} and p_{10} this is also the exact result to all orders, the higher order terms for the other four transitions are too complicated to be given here. The zeroth order terms in Eqs. (29) are those one would expect for independent atoms (namely the rates p_{10} and p_{01} for single V system multiplied by a factor 1, 2, or 3). For the first order terms it is important to note that the single systems interact via C_3 only if they are in a light period. Therefore the rates p_{01} and p_{10} are independent of C_3 while p_{12} and p_{21} have the same first order term as the corresponding rates for two V systems (in the intensity period I_2 the three V systems behave like two V systems in the period I_2 plus an additional noninteracting system). In the rates p_{23} and p_{32} the first order term is just twice the first order term of p_{21} and p_{12}. This surprising property is due to the simplicity of the quasisteady state $\rho_{\mathrm{ss},3}$, namely all diagonal elements of this state have the same first order dependence. Figure 4 shows the transition rate p_{32} for three V systems to first and to second order in C_3. The first order rate becomes negative for distances of about one-half to three quarters of a wavelength of the strong transition. By looking at the second order rate one can see that it is an artefact of the approximation. The rate with the dipole interaction included shows deviations of up to 100% from the rate for noninteracting atoms for distances of somewhat more than a wavelength λ_3.

By use of Eqs. (24), (21), and (23) the transition rates for three dipole-interacting D systems were also calculated, with the result

$$p_{01} = 3A_1, \quad p_{12} = 2A_1, \quad p_{23} = A_1, \tag{30a}$$

$$p_{10} = \frac{A_2\Omega_3^2}{A_3^2+2\Omega_3^2} \tag{30b}$$

and

$$p_{21} = 2\frac{A_2\Omega_3^2(A_3^2+2\Omega_3^2)}{(A_3^2+2\Omega_3^2)^2 + A_3^2(|C_3|^2 + 2A_3\,\mathrm{Re}\,C_3)} = \frac{2A_2\Omega_3^2}{A_3^2+2\Omega_3^2}\left[1 - 2\,\mathrm{Re}\,C_3\frac{A_3^3}{(A_3^2+2\Omega_3^2)^2}\right] + O(C_3^2), \tag{30c}$$

$$\begin{aligned} p_{32} &= \frac{3A_2\Omega_3^2[(A_3^2+2\Omega_3^2)^2 + A_3^2(|C_3|^2 + 2A_3\,\mathrm{Re}\,C_3)]}{(A_3^2+2\Omega_3^2)[(A_3^2+2\Omega_3^2)^2 + 3A_3^2(|C_3|^2 + 2A_3\,\mathrm{Re}\,C_3)] + 2A_3^2[|C_3|^2|A_3+C_3|^2 + (A_3^2+2A_3\,\mathrm{Re}\,C_3)^2]} \\ &= \frac{3A_2\Omega_3^2}{A_3^2+2\Omega_3^2}\left[1 - 4\,\mathrm{Re}\,C_3\frac{A_3^3}{(A_3^2+2\Omega_3^2)^2}\right] + O(C_3^2). \end{aligned} \tag{30d}$$

Compared to two D systems the transition rates show the same behavior as explained above for the three V systems. This is not surprising as the quasisteady states are identical and as the D systems also only interact via C_3 when they are

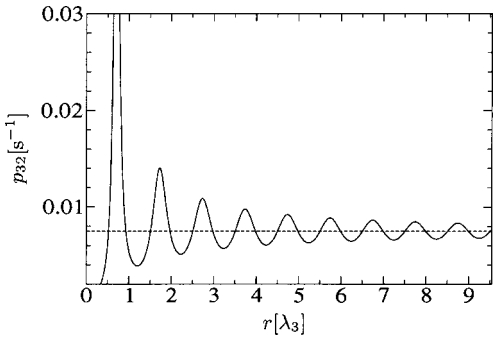

FIG. 5. Transition rate p_{32} for three dipole-interacting D systems. Dashed line, independent systems. Parameter values are $A_1=1\ s^{-1}$, $A_2=1\ s^{-1}$, $A_3=2\times10^8\ s^{-1}$, and $\Omega_2=10^7\ s^{-1}$.

in a light period. Figure 5 shows the exact transition rate p_{32} compared to the interaction free case. For distances of about a wavelength, p_{32} deviates up to 75% from the rate without interaction. The first peak at about 0.7 wavelengths even reaches a maximum of seven times the rate for independent atoms. For such small distances, however, one would have to check the validity of the model (namely, that in a particular intensity period most of the population is in a specific subspace). Also one must keep in mind that all the experiments cited here were performed at greater ion distances.

V. DOUBLE AND TRIPLE JUMP RATE

The physical quantity investigated in the experiments of Refs. [3,4,11–13] is the double jump rate. This is the rate at which jumps between periods of intensities that differ by twice the intensity of a single system occur within a small time interval. In Ref. [18] the double jump rate has been expressed in terms of the transition rates p_{ij} for two dipole-interacting V systems. The same will be done here for three systems. As one can calculate directly from Eqs. (19) and (23) there are no direct double jumps (i.e., $p_{ij}=0$ for $|i-j|>1$). A double jump is therefore defined as two successive jumps in the same direction which occur within a time which is smaller than a time window T_m so that they cannot be resolved. As there are four periods of different intensity in the fluorescence of three three-level systems, there are also four different possibilities for double jumps: From intensity zero to double intensity, from single intensity to threefold intensity, and vice versa. Therefore the whole double jump rate n_DJ is the sum of rates for the four different possible double jumps,

$$n_\mathrm{DJ}=n_\mathrm{DJ}^{20}+n_\mathrm{DJ}^{31}+n_\mathrm{DJ}^{13}+n_\mathrm{DJ}^{02}. \tag{31}$$

We first derive the rate for jumps from zero to double intensity. Each period of zero intensity ends with one of single intensity. The probability that the latter period is shorter than T_m is given by

$$p_{T_1<T_\mathrm{m}}=1-e^{-(p_{10}+p_{12})T_\mathrm{m}}.$$

The branching ratio for the following period to be of double intensity is $p_{12}/(p_{10}+p_{12})$. With the mean number of intensity periods I_i per unit time denoted by n_i the rate n_DJ^{02} is given by

$$n_\mathrm{DJ}^{02}=n_0\frac{p_{12}}{p_{10}+p_{12}}(1-e^{-(p_{10}+p_{12})T_\mathrm{m}}). \tag{32}$$

Analogously one finds

$$n_\mathrm{DJ}^{31}=n_3\frac{p_{21}}{p_{21}+p_{23}}(1-e^{-(p_{21}+p_{23})T_\mathrm{m}}). \tag{33}$$

The remaining two rates are a little bit more complicated as the periods of intensity I_1 and I_2 can be followed by a period with either higher or lower intensity. The rates n_DJ^{20} and n_DJ^{13} have thus to be supplemented with the branching ratios $p_{21}/(p_{21}+p_{23})$ and $p_{12}/(p_{10}+p_{12})$, respectively, yielding

$$n_\mathrm{DJ}^{13}=n_1\frac{p_{12}}{p_{10}+p_{12}}\frac{p_{23}}{p_{21}+p_{23}}(1-e^{-(p_{21}+p_{23})T_\mathrm{m}}) \tag{34}$$

and

$$n_\mathrm{DJ}^{20}=n_2\frac{p_{21}}{p_{21}+p_{23}}\frac{p_{10}}{p_{10}+p_{12}}(1-e^{-(p_{10}+p_{12})T_\mathrm{m}}). \tag{35}$$

Using the the relations

$$n_0=\frac{p_{10}}{p_{10}+p_{12}}n_1,\quad n_3=\frac{p_{23}}{p_{21}+p_{23}}n_2 \tag{36a}$$

and

$$n_2=\frac{p_{12}}{p_{10}+p_{12}}n_1+n_3,\quad n_1=n_0+\frac{p_{21}}{p_{21}+p_{23}}n_2 \tag{36b}$$

the double jump rates can be simplified to

$$n_\mathrm{DJ}^{02}=n_\mathrm{DJ}^{20}=n_1\frac{p_{10}p_{12}}{(p_{10}+p_{12})^2}(1-e^{-(p_{10}+p_{12})T_\mathrm{m}}) \tag{37}$$

and

$$n_\mathrm{DJ}^{13}=n_\mathrm{DJ}^{31}=n_1\frac{p_{12}p_{23}}{(p_{21}+p_{23})(p_{10}+p_{12})}(1-e^{-(p_{21}+p_{23})T_\mathrm{m}}). \tag{38}$$

We denote the mean durations of the intensity periods by T_i and note that

$$T_0=\frac{1}{p_{01}},\quad T_1=\frac{1}{p_{10}+p_{12}},\quad T_2=\frac{1}{p_{21}+p_{23}},\quad T_3=\frac{1}{p_{32}}. \tag{39}$$

In addition they fulfill

$$\sum_{i=0}^{3}n_iT_i=1. \tag{40}$$

The averaging window T_m is much smaller than the mean durations of the intensity periods. Therefore the exponential can be expanded and with Eq. (31) one gets

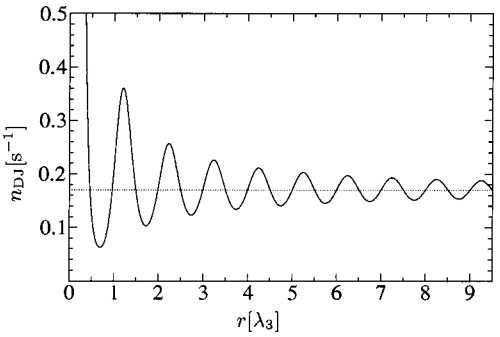

FIG. 6. Double jump rate n_{DJ} for three dipole-interacting V systems. Solid line, n_{DJ} up to second order in C_3. Dotted line, independent systems. Time window $T_m = 10^{-3}$ s. Other parameter values as in Fig. 4.

$$n_{DJ} = 2n_1 \frac{p_{12}(p_{10}+p_{23})}{p_{10}+p_{12}} T_m. \tag{41}$$

Using Eqs. (36a), (39) and (40) we finally obtain

$$n_{DJ} = 2\frac{p_{01}p_{21}p_{32}(p_{01}+p_{12})}{p_{21}p_{32}(p_{01}+p_{10})+p_{01}p_{12}(p_{23}+p_{32})} T_m \tag{42}$$

as the double jump rate for three of either three-level systems. A similar calculation yields for the triple jump rate

$$n_{TJ} = 2\frac{p_{01}p_{10}p_{12}p_{21}p_{23}p_{32}}{p_{21}p_{32}(p_{01}+p_{10})+p_{01}p_{12}(p_{23}+p_{32})} T_m^2. \tag{43}$$

Note that the defining time window T_m enters quadratically in this case. Figures 6 and 7 show plots of n_{DJ} for the V systems and the D systems, respectively, whereas Figs. 8 and 9 show plots of the triple jump rate n_{TJ} for both systems. For the D systems the exact values for the p_{ij} are used whereas for the V systems only the expanded expressions up to second order in C_3 are used since p_{23} and p_{23} could not be calculated exactly for the V systems. For the V systems there are cooperative effects of up to 110% for the double jump rate n_{DJ} and 170% for the triple jump rate n_{TJ} for distances of somewhat more than a wavelength of the strong transition. For the same distance range the D system shows cooperative effects of up to 150% for both n_{DJ} and n_{TJ}. The first peak at three quarters of a wavelength reaches 16 times the value for

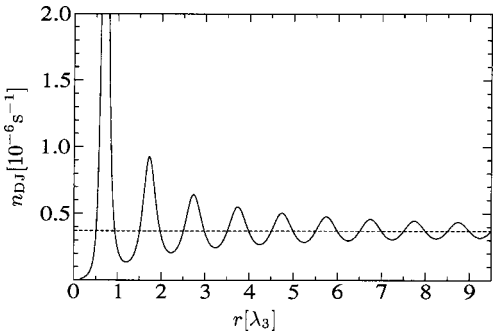

FIG. 7. Double jump rate n_{DJ} for three dipole-interacting D systems. Dashed line, independent systems. Time window $T_m = 5 \times 10^{-3}$ s. Other parameter values as in Fig. 5.

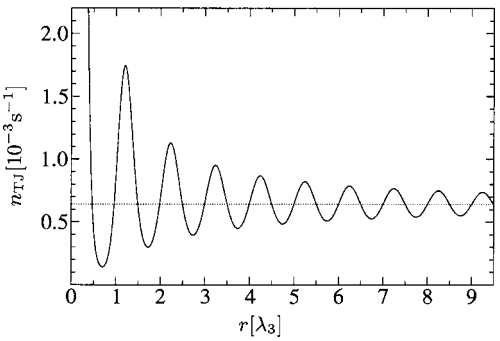

FIG. 8. Triple jump rate n_{TJ} for three dipole-interacting V systems. Solid line, n_{TJ} up to second order in C_3. Dotted line, independent systems. Parameter values as in Fig. 6.

independent systems for both rates. For distances of about 10 wavelengths cooperative effects of 15% are still present for both systems. In the case of the D system, which models the level configuration of the Hg^+ ions used in the experiments of Refs. [13,26], large cooperative effects only appear if the Rabi frequency Ω_3 is smaller than the Einstein coefficient A_3. So, for the experimental parameters (i.e., $\Omega_3 > A_3$ and $r/\lambda_3 \approx 15$) the effects are negligible, in agreement with the experimental results.

VI. CONCLUSIONS

We have investigated the effect of the dipole-dipole interaction on three three-level systems showing macroscopic light and dark periods in their fluorescence. This was done for the V and the D configuration, respectively. The latter models the effective level configuration of the Hg^+ ions in the experiments of Refs. [13,26]. We have explicitly calculated the transition rates between the different intensity periods for both configurations. In addition, the double and triple jump rates have been derived from these transition rates. Both systems show the same first order dependency on the coupling parameter C_3, leading to an enhancement in the cooperative effects by a factor of 2 for the transition rate p_{32}. This leads to cooperative effects of about 100% compared to the value for independent systems for interatomic distances of somewhat more than a wavelength of the strong transition.

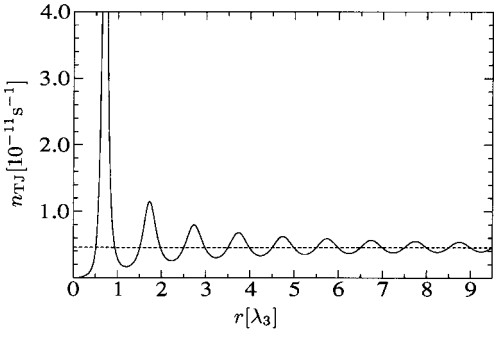

FIG. 9. Triple jump rate n_{TJ} for three dipole-interacting D systems. Dashed line, independent systems. Parameter values as in Fig. 7.

For the double and triple jump rates even larger cooperative effects can be seen. For three D systems the first peak at about three quarters of a wavelength is seven times higher for p_{32} and 16 times higher for n_{DJ} and n_{TJ} than for independent atoms.

Although we did not treat the four-level system of Ref. [20] here, which models the Ba^+ ions of Refs. [3,4], it is still possible to arrive at some conclusions on this experiment from our results for the three-level systems. As was pointed out in Ref. [20], the results for two D systems and two four-level systems are very similar, in particular in their first order term in C_3. It is therefore very likely that the cooperative effects for three four-level systems are also only enhanced by a factor of about 2, and since the effects for two four-level systems were already negligibly small one can expect a similar behavior also for three of such systems.

[1] See the references in Ref. [18].
[2] For references cf., e.g., Ref. [17].
[3] T. Sauter, R. Blatt, W. Neuhauser, and P. E. Toschek, Opt. Commun. **60**, 287 (1986).
[4] T. Sauter, Ph.D thesis, Universität Hamburg, 1987.
[5] B. H. W. Hendriks and G. Nienhus, J. Mod. Opt. **35**, 1331 (1988).
[6] M. Lewenstein and J. Javanainen, Phys. Rev. Lett. **59**, 1289 (1987).
[7] M. Lewenstein and J. Javanainen, IEEE J. Quantum Electron. **42**, 1403 (1988).
[8] G. S. Agarwal, S. V. Lawande, and R. D'Souza, IEEE J. Quantum Electron. **24**, 1413 (1988).
[9] S. V. Lawande, Q. V. Lawande, and B. N. Jagatap, Phys. Rev. A **40**, 3434 (1989).
[10] C. R. Fu and C. D. Gong, Phys. Rev. A **45**, 5095 (1992).
[11] D. J. Berkeland, D. A. Raymondson, and V. M. Tassin, physics/0304013.
[12] R. C. Thompson, D. J. Bates, K. Dholakia, D. M. Segal, and D. C. Wilson, Phys. Scr. **46**, 285 (1992).
[13] W. M. Itano, J. C. Bergquist, and D. J. Wineland, Phys. Rev. A **38**, 559 (1988).
[14] M. Block, O. Rehm, P. Seibert, and G. Werth, Eur. Phys. J. D **7**, 461 (1999).
[15] C. J. S. Donald, D. M. Lucas, P. A. Barton, M. J. McDonnell, J. P. Stacey, D. A. Stevens, D. N. Stacey, and A. M. Steane, Europhys. Lett. **51**, 388 (2000).
[16] C. Skornia, J. von Zanthier, G. S. Agarwal, E. Werner, and H. Walther, Phys. Rev. A **64**, 053803 (2001).
[17] A. Beige, and G. C. Hegerfeldt, Phys. Rev. A **59**, 2385 (1999).
[18] S. Addicks, A. Beige, M. Dakna, and G. C. Hegerfeldt, Eur. Phys. J. D **15**, 393 (2001).
[19] T. Sauter, W. Neuhauser, R. Blatt, and P. E. Toschek, Phys. Rev. Lett. **57**, 1696 (1986).
[20] V. Hannstein and G. C. Hegerfeldt, Phys. Rev. A **68**, 043826 (2003).
[21] C. Skornia, J. von Zanthier, G. S. Agarwal, E. Werner, and H. Walther, Europhys. Lett. **56**, 665 (2001).
[22] G. C. Hegerfeldt, Phys. Rev. A **47**, 449 (1993).
[23] G. C. Hegerfeldt and T. S. Wilser, in *Classical and Quantum Systems*, Proceedings of the Second International Wigner Symposium, July 1991, edited by H. D. Doebner, W. Scherer, and F. Schroeck (World Scientific, Singapore, 1992), p. 104; G. C. Hegerfeldt, Phys. Rev. A **47**, 449 (1993); G. C. Hegerfeldt and D. G. Sondermann, Quantum Semiclassic. Opt. **8**, 121 (1996). For a review cf. M. B. Plenio and P. L. Knight, Rev. Mod. Phys. **70**, 101 (1998).The quantum jump approach is essentially equivalent to the Monte Carlo wave-function approach of J. Dalibard, Y. Castin, and K. Mølmer, Phys. Rev. Lett. **68**, 580 (1992), and to the quantum trajectories of H. Carmichael, *An Open Systems Approach to Quantum Optics*, Lecture Notes in Physics m18 (Springer, Berlin, 1993).
[24] A. Beige and G. C. Hegerfeldt, Phys. Rev. A **58**, 4133 (1998).
[25] A. Beige and G. C. Hegerfeldt, J. Phys. A **30**, 1323 (1997).
[26] W. M. Itano, J. C. Bergquist, R. G. Hulet, and D. J. Wineland, Phys. Rev. Lett. **59**, 2732 (1987).